ISSN 0915-6364

NATIONAL INSTITUTE FOR FUSION SCIENCE

Unified Analytic Formula for Physical Sputtering Yield at Normal Ion Incidence

R. K. Janev, Yu.V. Ralchenko, T. Kenmotsu

(Received - Mar. 19, 2001)

NIFS-DATA-62 Apr. 2001

RESEARCH REPORT
NIFS-DATA Series

TOKI, JAPAN

Unified Analytic Formula for Physical Sputtering Yield at Normal Ion Incidence

R. K. Janev[*†], Yu. V. Ralchenko[*‡], T. Kenmotsu[*]

Abstract

A new analytic representation of the physical sputtering yield at normal ion incidence is derived, providing a unified description of the sputtering data at all impact energies and for all ion-monoatomic-solid-target combinations. The reduced sputtering yield $\tilde{Y}$ is expressed in terms of only one energy parameter η. The function $\tilde{Y}(\eta)$ has a simple analytic form and describes all the available experimental and calculated data with an rms deviation of 32%. Tables of the parameters entering the analytic formula for $\tilde{Y}(\eta)$ are provided for a number of ions and monoatomic solids of interest in fusion and other research fields.

PACS number(s): 79.20.R

Keywords: physical sputtering; normal incidence; scaling formula.

[*]National Institute for Fusion Science, Oroshi-cho, Toki-shi, Gifu-ken 509-5292, Japan
[†]Macedonian Academy of Sciences and Arts, P.O.Box 482, 91000 Skopje, Macedonia
[‡]Faculty of Physics. Weizmann Institute of Science, Rehovot 76100. Israel

1 Introduction

The existing analytic representation of physical sputtering yield $Y(E)$ for normal ion incidence on solids [1, 2, 3, 4, 5] are all based on the factorization

$$Y(E, E_{th}, E_{TF}) = Q\,\varphi\left(\frac{E}{E_{th}}\right) s_n(\varepsilon), \qquad \varepsilon = \frac{E}{E_{TF}}. \tag{1}$$

where E is the projectile ion energy, E_{th} is the threshold energy and E_{TF} is the Thomas-Fermi energy, defined as (see, e.g., [2]):

$$E_{TF}(eV) = 30.74\,\frac{M_1}{M_2}\left(1+\frac{M_2}{M_1}\right) \times Z_1 Z_2 \left(Z_1^{2/3}+Z_2^{2/3}\right)^{1/2}, \tag{2}$$

where $M_1(M_2)$ and $Z_1(Z_2)$ are the mass and nuclear charge of the projectile ion (target atom), respectively.

The function $s_n(\varepsilon)$ in Eq.(1) represents the nuclear stopping cross section and its specific form depends on the interaction potential used for the ion-target atom interaction. The electronic stopping contribution to Y is usually included in Q in an implicit way, when Q is treated as a fitting parameter in (1) [1, 2, 3], or explicitly [4, 5]. There is, at present, no clear physical basis for determining the function $\varphi(E/E_{th})$ (see, however, [4]) and its form is usually determined empirically to provide the best description of the data in the threshold region. In the well-known Bohdansky formula [1] and its modified version [2], $\varphi(x)$ is taken in the form

$$\varphi_B(x) = \left(1-\frac{1}{x^{2/3}}\right)\left(1-\frac{1}{x}\right)^2, \qquad x = \frac{E}{E_{th}}. \tag{3}$$

while Yamamura and his coworkers [4, 5] use

$$\varphi_{Ya}(x) = \left(1-x^{-1/2}\right)^s \tag{4}$$

with $s = 2.5$ or $s = 2.8$. It should be noted that the functions $\varphi_B(x)$ and $\varphi_{Ya}(x)$ both tend to zero when x tends to one (threshold), and they tend to one when $x \gg 1$.

If both Q and E_{th} are treated as fitting parameters in Eq.(1), then it has been shown in Ref. [2] that determining $s_n(\varepsilon)$ on a basis of the Kr-C interaction potential (rather than from the Thomas-Fermi potential, as was originally done by Bohdansky [1]) provides a more successful fit to the experimental data for all projectile-monoatomic target combinations. The revised Bohdansky sputtering formula [2], thus, uses $s_n(\varepsilon)$ in the form

$$s_n(\varepsilon) = \frac{0.5\ln(1+1.2288\varepsilon)}{\varepsilon+0.1728\varepsilon^{0.5}+0.008\varepsilon^{0.1504}}. \tag{5}$$

The factorization (1) of sputtering yield $Y(E)$ is useful in the sense that it indicates that in the threshold region $Y(E)$ for all projectile-target combinations can be represented in a unified way in terms of the reduced energy parameter $x = E/E_{th}$ and the function $\varphi(x)$, while in the asymptotic region the parameter $\varepsilon = E/E_{TF}$ serves as appropriate reduced energy parameter with the

function $s_n(\varepsilon)$ describing the energy behavior of Y in a unified way (e.g., when Y is divided by Q). The appearance of the reduced energy parameters x and ε in the threshold and asymptotic regions, respectively, is natural since these parameters express the collision energy in terms of the characteristic potential interaction energy in the two regions (the surface binding energy E_s, related to E_{th}, and the Thomas-Fermi interaction energy E_{TF}, respectively). In the intermediate energy region, however, neither E_{th} nor E_{TF} can be considered as characteristic measures for the potential interaction energy in the system, in terms of which the collision energy can be expressed in a natural way. From this point of view, the factorization (1), while providing an adequate description of $Y(E)$ in the threshold and asymptotic regions, fails to do so in the intermediate energy range. This explains the need for so many fitting parameters in the functions $\varphi(x)$ and $s_n(\varepsilon)$ (eight, in the case of Bohdansky original and revised formulae) to describe the consistently smooth and uniform behavior of $Y(E)$.

In the present report we construct a generalized reduced energy parameter $\eta = \eta(E, E_{th}, E_{TF})$ which appropriately represents the ratio of dynamical and potential interaction forces in the intermediate energy range, and in the threshold and asymptotic regions goes over smoothly into the reduced energy parameters E/E_{th} and ε, respectively. The reduced energy parameter η allows one to introduce a reduced (scaled) sputtering yield $\tilde{Y}$ which depends only on η. The unified representation $\tilde{Y}(\eta)$ of sputtering yield can also be presented in an analytic form which describes the available experimental and calculated sputtering data for ion-monoatomic target collision systems with an accuracy well within their own uncertainties. A brief account of the derivation of $\tilde{Y}(\eta)$ was given elsewhere [6]. The purpose of the present report is to provide more details on the derivation of $\tilde{Y}(\eta)$ and describe the procedure of generating $Y(E)$ from the universal function $\tilde{Y}(\eta)$.

The organization of the report is as follows. In the next section we give the derivation of reduced sputtering yield and provide an analytic expression for $\tilde{Y}(\eta)$. In Section 3 we describe the procedure for calculating $Y(E)$ for any projectile-monoatomic target combination on the basis of reduced sputtering yield function $\tilde{Y}(\eta)$ and provide a table of the parameters entering $\tilde{Y}(\eta)$ for a quick calculation of $Y(E)$ for a number of ion-target combinations of interest to fusion and other research fields. In Section 4 we give some concluding remarks.

2 Derivation of Reduced Sputtering Yield Function $\tilde{Y}(\eta)$

We introduce the notation

$$\varepsilon = \frac{E}{E_{TF}}, \qquad \delta = \frac{E_{th}}{E_{TF}} \tag{6}$$

in terms of which the factorized sputtering yield of Eq. (1) can be written as

$$Y\left(\frac{\varepsilon}{\delta}, \varepsilon\right) = Q\ \varphi\left(\frac{\varepsilon}{\delta}\right)\ s_n(\varepsilon)\,. \tag{1'}$$

We further define the generalized energy parameter $\eta = \eta(E, E_{th}, E_{TF})$ by the expression

$$\eta = a\left(\frac{\varepsilon}{\delta} - 1\right) + b\left[\left(\frac{\varepsilon}{\delta}\right)^{\gamma} - 1\right] + 1, \quad (7)$$

where a, b and γ depend on δ, and the reduced sputtering yield

$$\tilde{Y}(\eta) = \frac{Y(E, E_{th}, E_{TF})}{Q\,G(\delta)} = \frac{Y(\varepsilon, \delta)}{Q\,G(\delta)}. \quad (8)$$

where $G(\delta)$ is a function of δ and Q is defined in a usual way (see, e.g., [2]) by the equation $Y^{>} = Q\,s_n(\varepsilon)$, $Y^{>}$ being the sputtering yield in the asymptotic region (so that Q is a constant). Instead of using this equation, Q is usually (see, e.g., [2, 3]), together with E_{th}, treated as a free fitting parameter for the entire $Y(E)$ and thus acquires a δ-dependence. Therefore, the ratio Y/Q, even in the asymptotic region, becomes dependent on δ. (For the majority of projectile-target combinations investigated so far, the variations of the parameters Q and δ are in the ranges $10^{-2} - 10^{-1}$ and $10^{-6} - 10^{-1}$, respectively.) The function $G(\delta)$ in Eq. (8) is determined from the condition that sputtering yields for the individual ion-solid collision pairs (with δ spanning the above range) have the same maximum value, $\tilde{Y}_m$. The dependence $G(\delta)$ is rather smooth and can be accurately represented by the function

$$G(\delta) = 0.85 + 4.0\exp\left(-2.94\,\delta^{3/5}\right). \quad (9)$$

The reduced sputtering yields $Y(\varepsilon, \delta)/QG(\delta)$ on the ε-scale now all have the same maxima but are mutually displaced due to their δ-dependence (see Fig.1) In order to eliminate the δ-dependence of reduced sputtering yield, we use the relation (7), which transforms the variable ε into η, and impose on the functions $a(\delta)$, $b(\delta)$ and $\gamma(\delta)$ the condition that all reduced yields $Y(\varepsilon, \delta)/QG(\delta)$ coincide with the reduced yield for $\delta = 1$. This condition determines uniquely the dependences $a(\delta)$, $b(\delta)$ and $\gamma(\delta)$ in the entire range of variation of δ. To a high degree of accuracy, the dependencies of a, b and γ on δ can be represented by the expressions

$$a(\delta) = 1.265\,\frac{\delta}{(0.18 + \delta^{2/3})}. \quad (10)$$

$$b(\delta) = 20.5\,\frac{\delta^{2/5}}{(1 + 112\delta)}, \quad (11)$$

$$\gamma(\delta) = 0.81\,\frac{(0.0051 + \delta^{4/5})}{(0.013 + \delta^{3/5})}. \quad (12)$$

The reduced sputtering yield representation $\tilde{Y}(\eta)$ is now completely defined.

With the functions $a(\delta)$, $b(\delta)$ and $\gamma(\delta)$ determined, we can now investigate the asymptotic behavior of η. It follows from Eq. (7) that in the threshold region, i.e. $\varepsilon/\delta = E/E_{th} \to 1$, $\eta \sim (E/E_{th})^{a+b\gamma}$. For all values of $\delta(\leqslant 1)$ the parameter γ is always less than one, and therefore in the high energy region the leading term in η is $a\varepsilon/\delta$. Furthermore, noting that $a \sim \delta$ (see Eq.(10)), it follows that $\eta \sim \varepsilon$ and the proportionality factor weakly depends on δ. Therefore, the

generalized reduced energy parameter η has the proper physical behavior in the threshold and asymptotic regions.

In order to verify (and demonstrate) the effectiveness of the unified representation $\tilde{Y}(\eta)$ of the sputtering yield, we first show in Fig. 2 the experimental data collected in Ref. [2] in the ordinary $Y(E)$ representation. Two features should be noted on this graph. First, the data for the same projectile-target combination are considerably scattered and, second, the value of the sputtering yield for different ion-solid collision pairs at given energy can vary by as much as five orders of magnitude. In Fig. 3, the same data are plotted in the $\tilde{Y}(\eta)$ representation. It is apparent that the data for different projectile-target combinations tend to follow a single line, while their original uncertainties remain unchanged. This indicates that the reduced sputtering yield $\tilde{Y}(\eta)$, as defined by Eqs. (7)-(12) , provides a unified representation of sputtering data for all considered projectile-target combinations. Figures 4 and 5 give a similar comparison of the $Y(E)$ and $\tilde{Y}(\eta)$ representations for the sputtering data calculated with the Monte Carlo simulation code TRIM.SP and given also in Ref. [2]. The smaller dispersion of $\tilde{Y}(\eta)$ TRIM.SP data in Fig. 5 with respect to that of experimental ones in Fig. 3 reflects the fact that TRIM.SP data have a higher consistency among each other than the experimental ones (see Ref. [2]).

The smooth overall behavior of the reduced sputtering yield data on Figs. 3 and 5 suggests that these data can be fitted to a simple analytic function $\tilde{Y}(\eta)$ in the entire η-region. The function $\tilde{Y}(\eta)$ should obviously possess the following properties

$$\tilde{Y}(\eta) \rightarrow g(\eta) \rightarrow 0, \text{ for } \eta \rightarrow 1 \qquad (13)$$

$$\tilde{Y}(\eta) \rightarrow f(\eta) \sim \frac{\ln \eta}{\eta}, \text{ for } \eta \rightarrow \infty. \qquad (14)$$

The condition (13) expresses the mere fact of existence of a threshold ($\eta = 1$) for the sputtering process, while the property (14) is consistent with the high-energy behaviour of Bohdansky's formula. As it was mentioned in the Introduction, there is, at present, no clear physical basis for determining more specifically the form of the function $g(\eta)$. We, therefore, adopt a pragmatic approach and from the multitude of possible forms for $g(\eta)$ satisfying the condition (13),we choose the simplest one which provides a good description of the data behavior in the threshold region. Exploration of the possible functional forms for $g(\eta)$ and $f(\eta)$ has led to the conclusion that the function

$$\tilde{Y}(\eta) = \left(1 - \frac{1}{\eta}\right)^{\alpha} \left[\frac{A \ln \eta}{\eta} + \frac{B}{\eta^2}\right] \qquad (15)$$

has the simplest and most compact form which satisfies the conditions (13) and (14) and provides equally good fit to the data as other functions with more fitting parameters. A least-square fit of the experimental data on Fig. 3 gives for the coefficients α, A and B the values $\alpha = 3$, $A = 0.451$, $B = 0.183$, with an rms deviation of 33%. The least-square fit

of the TRIM.SP data in Fig. 5 with the function (15) gives $\alpha = 3$, $A = 0.414$, $B = 0.246$, with an rms deviation of 30%. We see that the values of the fitting parameters A and B are close for both sets of data. We therefore combine the two data sets into one (Fig. (6)) and then fit all data points with the function (15). The best fit is obtained with the parameters:

$$\alpha = 3, \quad A = 0.436, \quad B = 0.212 \qquad (16)$$

with an rms deviation of 32%. The solid curve in Fig. 6 represents the function $\tilde{Y}(\eta)$ with the parameters given by Eq. (16).

A distinct feature of the reduced sputtering yield $\tilde{Y}(\eta)$ is the simplicity of its analytic form, Eq. (15). This is to be contrasted with the complex expression for the reduced sputtering yield $Y/Q = \varphi(E/E_{th})\, s_n(\varepsilon) \equiv \bar{Y}_{rB}(\varepsilon, \delta)$ following from the revised Bohdansky formula, Eqs. (1)-(5). It can be remarked that the reduced revised Bohdansky sputtering yield formula $\bar{Y}_{rB}(\varepsilon, \delta)$ can also be written in terms of the scaled energy for η. From the procedure of determining the functions $a(\delta)$, $b(\delta)$ and $\gamma(\delta)$ it is clear that the η-scaled $\bar{Y}_{rB}$ can be obtained by setting $\delta = 1$ and replacing ε with η in $\bar{Y}_{rB}$, i.e.,

$$\begin{aligned} \tilde{Y}_{rB}(\eta) &= \bar{Y}_{rB}(\varepsilon \to \eta, \delta = 1) \\ &= \varphi(\eta)\, s_n(\eta). \end{aligned} \qquad (17)$$

The function $\tilde{Y}_{rB}(\eta)$ is shown in Fig. 6 by the dashed line. This function differs from $\tilde{Y}(\eta)$ only for very large values of η (about 15% for $\eta = 300$, for instance).

3 Determination of $Y(E)$ from Reduced Sputtering Yield Function $\tilde{Y}(\eta)$

The reduced sputtering yield function $\tilde{Y}(\eta)$ given by Eqs. (15)-(16), represents the sputtering yield for all projectile-monoatomic solid combinations in a unified form. Therefore, it can be used to determine the sputtering $Y(E)$ for any projectile-elemental target combination by using the relation (8) and Eqs. (7), (9)-(12). Besides the collision energy E, the only input parameters in these relations are Q and $\delta = E_{th}/E_{TF}$. The Thomas-Fermi energy E_{TF}, expressed in terms of the nuclear charge and mass of projectile ion (Z_1, M_1) and target atom (Z_2, M_2), is given by Eq. (2).

The parameters Q and E_{th} can also be expressed in terms of $Z_{1,2}$, $M_{1,2}$ by the relations [2]:

$$\begin{aligned} Q E_s^{2/3} &= 0.278\,(Z_1 Z_2)^{2/3} \left(Z_1^{2/3} + Z_2^{2/3}\right)^{1/3} \\ &\quad \times \left(\frac{M_2}{M_1}\right)^{1/6} \frac{1}{1 + \frac{M_2}{M_1}}, \end{aligned} \qquad (18)$$

$$\frac{E_{th}}{E_s} = 7.0 \left(\frac{M_2}{M_1}\right)^{-0.54} + 0.15 \left(\frac{M_2}{M_1}\right)^{1.12} \qquad (19)$$

where E_s is the surface binding energy in units of eV [2, 7]. The relations (18) and (19) have been obtained in Ref. [2] as best fits of the values for Q and E_{th} determined by fitting

the experimental and TRIM.SP data to the revised Bohdansky sputtering formula, Eqs. (1)-(5). It should be noted, however, that the dispersion of the experimental and TRIM.SP Q and E_{th} data with respect to the best-fit functions (18) and (19), respectively, is fairly large and can lead to errors in the calculated $Y(E)$ yield up to a factor of two or more.

In order to facilitate the calculation of $Y(E)$ from $\tilde{Y}(\eta)$ by using the relation

$$Y(E) = QG(\delta)\tilde{Y}(\eta) \equiv \tilde{Q}(\delta)\tilde{Y}(\eta) \quad (20)$$

we have calculated the parameters δ, $\tilde{Q}(\delta)$, $a(\delta)$, $b(\delta)$, and $\gamma(\delta)$ for a number of projectile-monoatomic target combinations which are of interest in fusion and other research fields. The corresponding Q and E_{th} values were taken from the fits of experimental data (and where unavailable, from TRIM.SP data) to the revised Bohdansky formula [2], which in its η-scaled form is consistent with the $\tilde{Y}(\eta)$ function (see the preceding section). The values of the above parameters for the selected ion-solid collision pairs, together with the value of E_{th}, are given in Table 1. We note also that ε/δ appearing in the expression for η, Eq. (7), can be replaced by E/E_{th}.

4 Conclusions

In the present work we have derived a unified analytic representation of physical sputtering yield for normal ion incidence by introducing the generalized reduced energy parameter η and the reduced sputtering yield $\tilde{Y}$. The generalized reduced (scaled) energy parameter η describes adequately the ratio of dynamical and potential interactions in the system in the entire region of its variation, and in the threshold and asymptotic regions goes over into its well-known forms. The reduced (scaled) sputtering yield function $\tilde{Y}(\eta)$, given by Eqs. (15)-(16), represents the experimental and computer simulation data well within their own uncertainties. The function $\tilde{Y}(\eta)$ has also proper physical behavior in the threshold and asymptotic regions. The established unified representation of the sputtering yield for all ion-monoatomic solid target combinations expresses the fact that the underlying physical mechanisms governing the sputtering phenomenon are, generally speaking, the same in all ion-solid collision systems. This fact is also revealed by the success of Monte Carlo simulation codes (e.g., TRIM.SP and ACAT) in describing the sputtering process. The single reduced sputtering yield function $\tilde{Y}(\eta)$ can be used to generate the sputtering yield $Y(E)$ in ion-monoatomic target collision systems for which data are not available.

References

[1] J. Bohdansky, Nucl. Instrum. Methods B2 (1984) 587.

[2] W. Eckstein, C. Garcia-Rosales, J. Roth and W. Ottenberger, Institute for Plasma Physics (Garching) Report IPP 9/82 (1993).

[3] E. W. Thomas, R. K. Janev, J. Botero, J. J. Smith and Y. Qiu, IAEA Report INDC(NDS)-287 (1993).

[4] Y. Yamamura, N. Matsunami and N. Itoh, Radiat. Eff. 71 (1983) 65.

[5] Y. Yamamura and H. Tawara, At. Data and Nucl. Data Tables 62 (1996) 149.

[6] R. K. Janev, Yu. V. Ralchenko, T. Kenmotsu and K. Hosaka, J. Nucl. Mat. (submitted, 2001).

[7] R. Hultgren et al., *Selected Values of Thermodynamic Properties of Elements* (Am. Soc. Metals, Metals Park, OH, 1973).

Figure Captions.

Figure 1. Reduced sputtering yield $Y(\varepsilon, \delta)/QG(\delta)$ vs. ε for different values of parameter δ.

Figure 2. Experimental data on normal incidence sputtering yield [2].

Figure 3. Reduced sputtering yield and the best least-square fit for experimental data of Ref. [2].

Figure 4. Theoretical (TRIM.SP) data on normal incidence sputtering yield [2].

Figure 5. Reduced sputtering yield and the best least-square fit for theoretical (TRIM.SP) data of Ref. [2].

Figure 6. Reduced sputtering yield and the best least-square fit for experimental and theoretical (TRIM.SP) data of Ref. [2].

Table 1. The parameters for calculation of the reduced energy η (Eq. (7)) and sputtering yield Y (Eq. (20)) for a number of projectile(A)-target combinations.

A	E_{th}	δ	a	b	γ	Q
Target: **Be**						
H	3.51e+01	1.371e-01	3.890e-01	5.661e-01	5.351e-01	1.964e-01
D	2.62e+01	9.291e-02	3.052e-01	6.948e-01	4.941e-01	5.106e-01
He	4.45e+01	6.181e-02	2.325e-01	8.498e-01	4.547e-01	1.580e+00
Be	2.30e+01	1.042e-02	5.787e-02	1.524e+00	3.239e-01	3.200e+00
Ne	4.02e+01	3.771e-03	2.336e-02	1.546e+00	2.795e-01	8.465e+00
Ar	4.81e+01	1.306e-03	8.604e-03	1.255e+00	2.570e-01	1.372e+01
Target: **C**						
H	2.73e+01	6.578e-02	2.426e-01	8.249e-01	4.605e-01	8.401e-02
D	2.43e+01	5.436e-02	2.126e-01	9.022e-01	4.431e-01	1.950e-01
He	3.02e+01	2.778e-02	1.293e-01	1.189e+00	3.878e-01	1.427e+00
C	3.50e+01	6.153e-03	3.645e-02	1.584e+00	2.981e-01	5.196e+00
Ne	6.96e+01	4.995e-03	3.020e-02	1.578e+00	2.895e-01	7.020e+00
Ar	7.11e+01	1.552e-03	1.015e-02	1.314e+00	2.591e-01	1.411e+01
Target: **Fe**						
H	6.70e+01	2.634e-02	1.241e-01	1.212e+00	3.838e-01	1.636e-01
D	4.50e+01	1.737e-02	8.895e-02	1.376e+00	3.547e-01	4.725e-01
He	2.60e+01	4.713e-03	2.865e-02	1.574e+00	2.873e-01	1.884e+00
Fe	3.58e+01	2.056e-04	1.417e-03	6.715e-01	2.634e-01	6.544e+01

Table 1 (continued).

A	E_{th}	δ	a	b	γ	Q
Target: **Cu**						
H	5.10e+01	1.743e-02	8.919e-02	1.374e+00	3.549e-01	2.519e-01
D	3.30e+01	1.110e-02	6.113e-02	1.510e+00	3.274e-01	9.625e-01
He	1.80e+01	2.860e-03	1.808e-02	1.492e+00	2.713e-01	3.791e+00
Ar	2.70e+01	2.558e-04	1.759e-03	7.289e-01	2.608e-01	6.673e+01
Cu	2.66e+01	1.184e-04	8.211e-04	5.437e-01	2.709e-01	8.826e+01
Target: **Mo**						
H	1.99e+02	4.217e-02	1.771e-01	1.010e+00	4.210e-01	2.740e-02
D	9.00e+01	1.888e-02	9.517e-02	1.345e+00	3.602e-01	9.742e-02
T	6.00e+01	1.246e-02	6.741e-02	1.481e+00	3.340e-01	3.840e-01
He	4.75e+01	4.776e-03	2.900e-02	1.575e+00	2.878e-01	7.170e-01
Ne	2.80e+01	4.381e-04	2.984e-03	8.863e-01	2.558e-01	1.217e+01
Ar	3.25e+01	2.268e-04	1.562e-03	6.968e-01	2.622e-01	3.746e+01
Mo	5.51e+01	1.034e-04	7.176e-04	5.158e-01	2.729e-01	7.681e+01
Target: **W**						
H	4.29e+02	4.346e-02	1.811e-01	9.966e-01	4.236e-01	2.383e-02
D	1.78e+02	1.793e-02	9.129e-02	1.364e+00	3.568e-01	7.020e-02
T	1.29e+02	1.293e-02	6.957e-02	1.471e+00	3.362e-01	2.662e-01
He	1.07e+02	5.251e-03	3.160e-02	1.581e+00	2.915e-01	4.812e-01
Ne	2.60e+01	2.183e-04	1.504e-03	6.868e-01	2.627e-01	1.275e+01
Ar	3.65e+01	1.480e-04	1.024e-03	5.925e-01	2.678e-01	3.640e+01
W	5.90e+01	2.952e-05	2.063e-04	3.150e-01	2.899e-01	1.491e+02

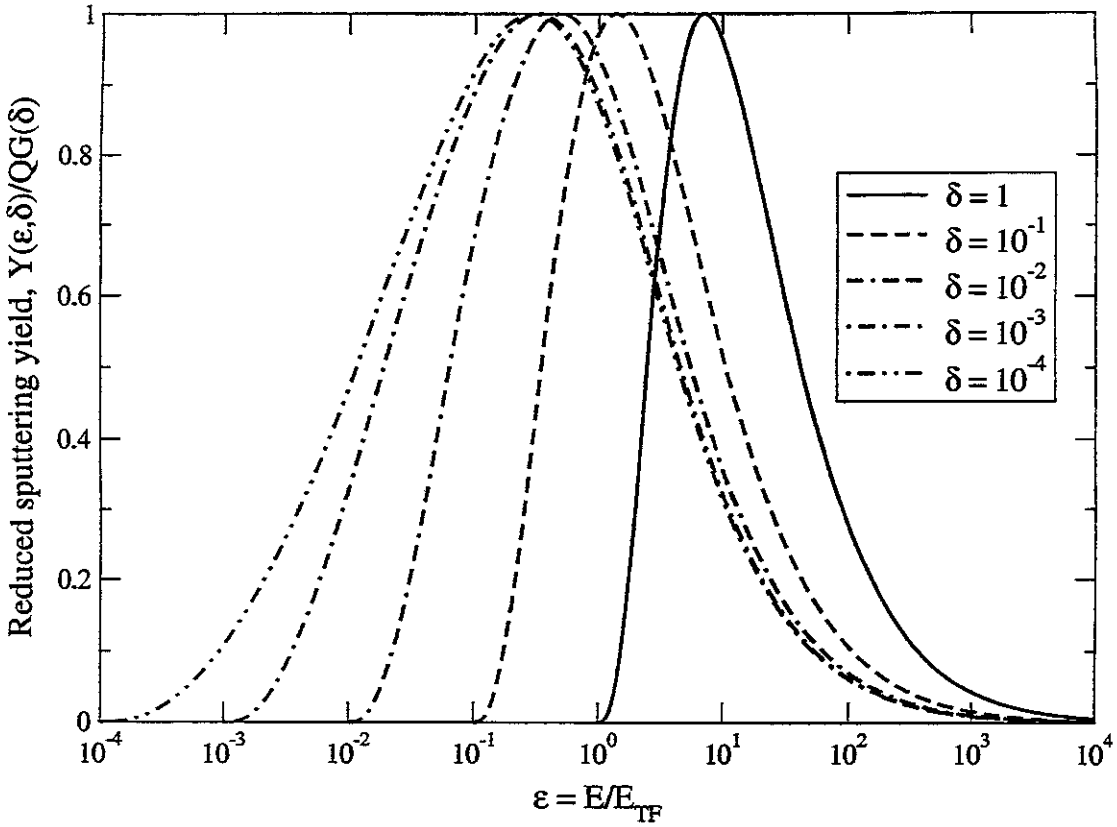

Figure 1. Reduced sputtering yield Y(ε , δ)/QG(δ) vs. ε for different values of parameter δ .

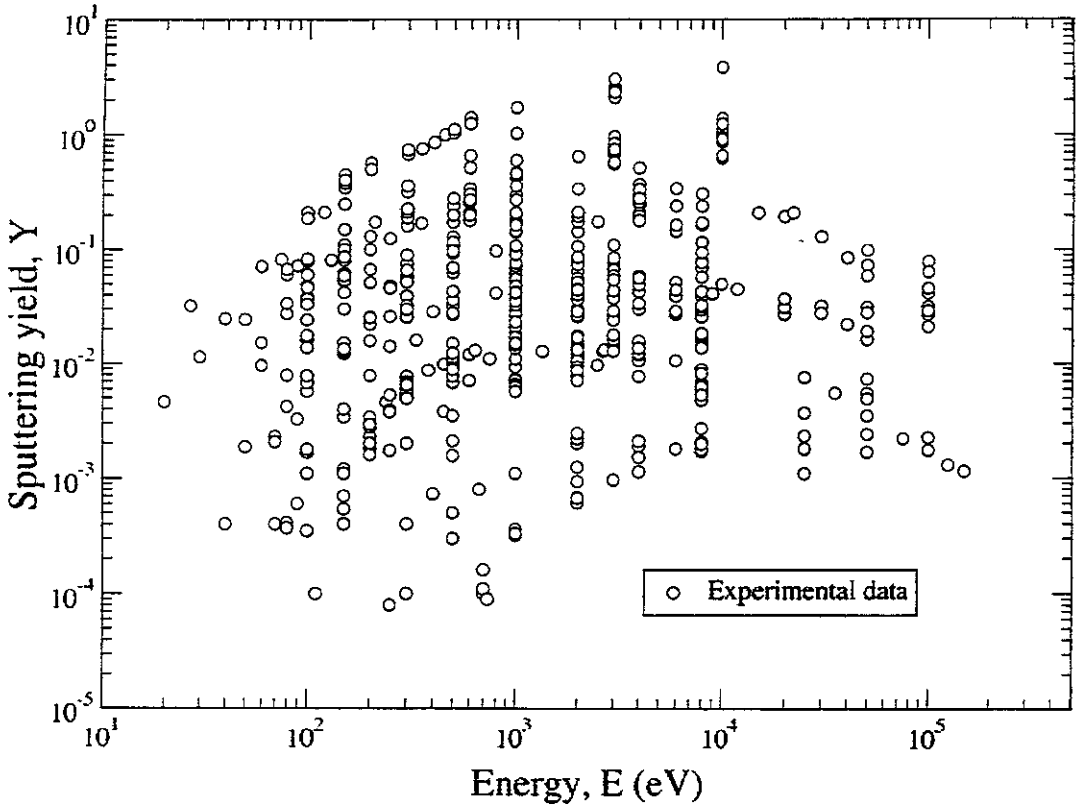

Figure 2. Experimental data on normal incidence sputtering yield [2].

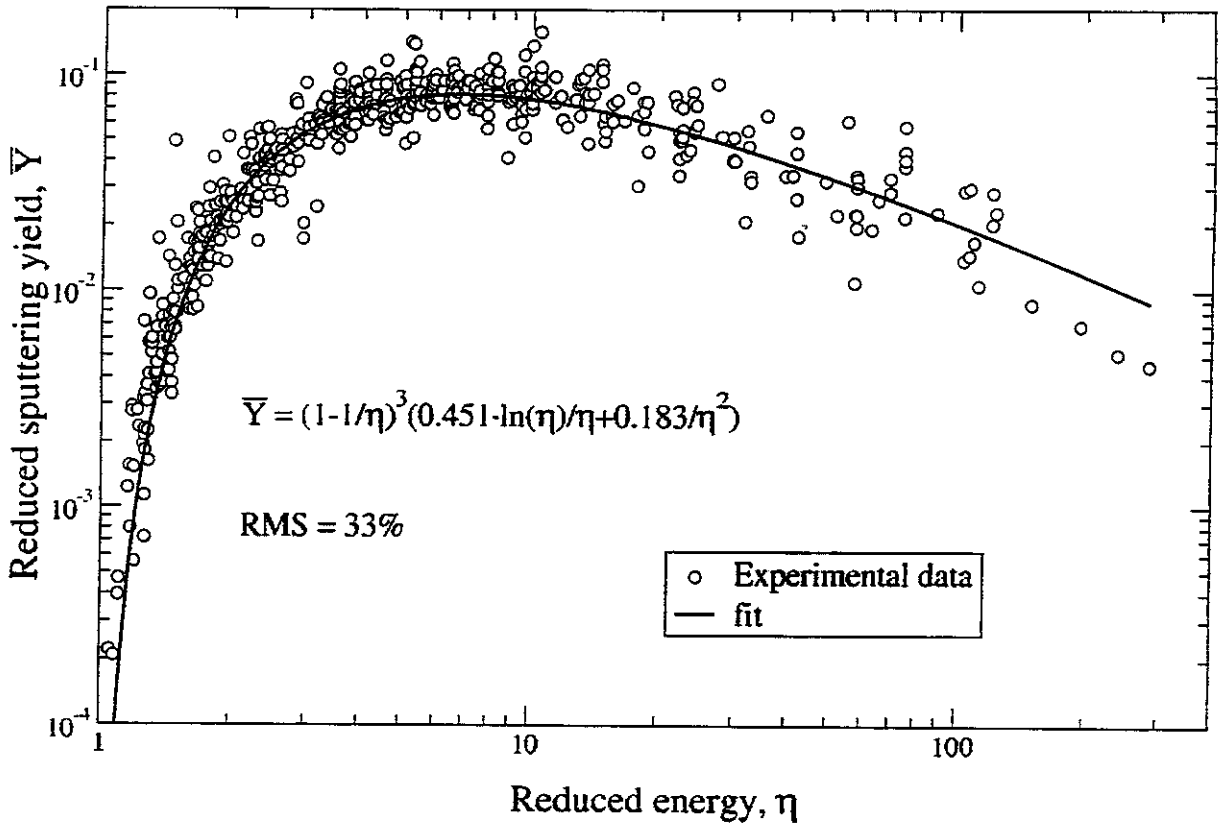

Figure 3. Reduced sputtering yield and the best least-square fit for experimental data of Ref. [2].

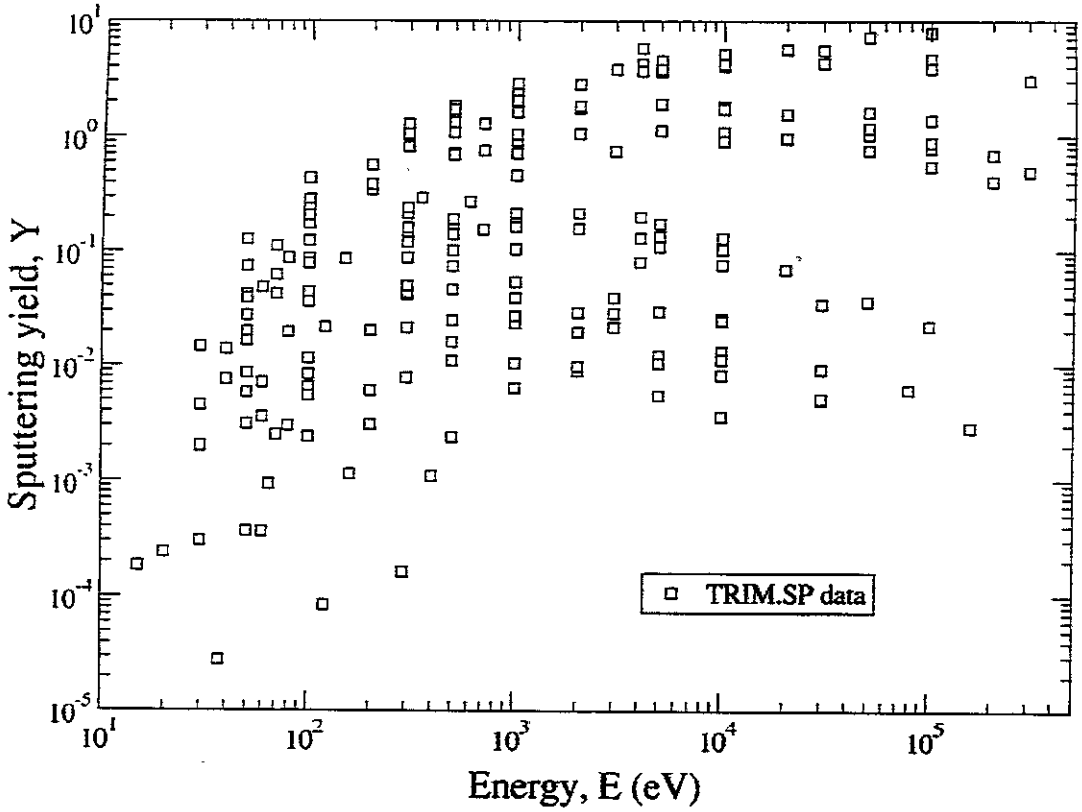

Figure 4. Theoretical(TRIM.SP) data on normal incidence sputtering yield [2].

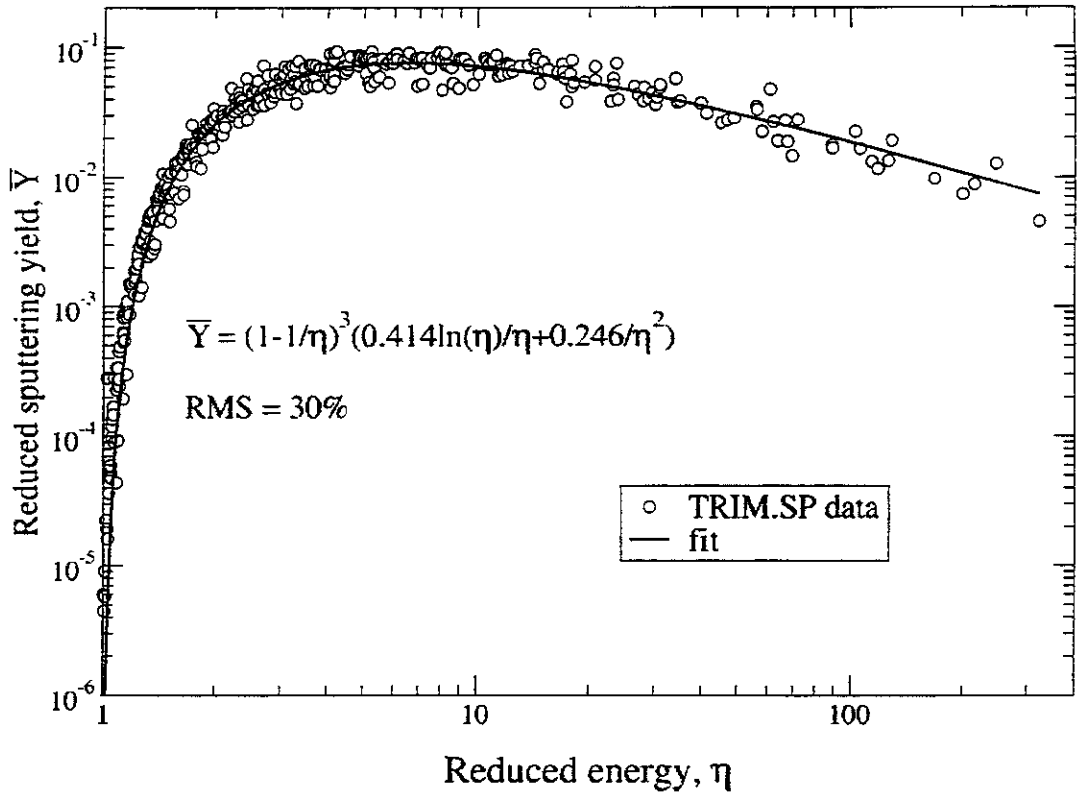

Figure 5. Reduced sputtering yield and the best least-square fit for theoretical (TRIM.SP) data of Ref. [2].

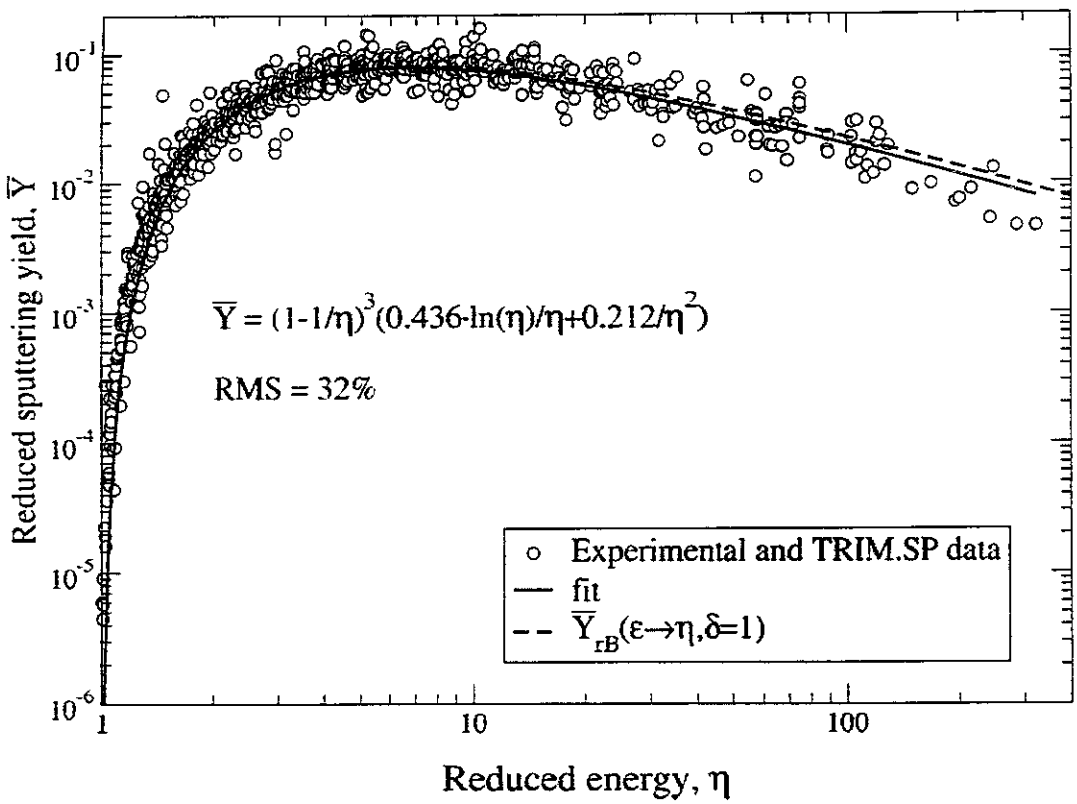

Figure 6. Reduced sputtering yield and the best least-square fit for experimental and theoretical (TRIM.SP) data of Ref. [2]

Recent Issues of NIFS-DATA Series

NIFS-DATA-42 H. Tawara,
Bibliography on Electron Transfer Processes in Ion-ion / Atom / Molecule Collisions -Updated 1997 -;
May 1997

NIFS-DATA-43 M. Goto and T. Fujimoto,
Collisional-radiative Model for Neutral Helium in Plasma: Excitation Cross Section and Singlet-triplet Wavefunction Mixing; Oct. 1997

NIFS-DATA-44 J. Dubau, T. Kato and U.I. Safronova,
Dielectronic Recombination Rate Coefficients to the Excited States of CI From CII; Jan. 1998

NIFS-DATA-45 Y. Yamamura, W. Takeuchi and T. Kawamura,
The Screening Length of Interatomic Potential in Atomic Collisions; Mar. 1998

NIFS-DATA-46 T. Kenmotsu, T. Kawamura, T. Ono and Y. Yamamura,
Dynamical Simulation for Sputtering of B4C; Mar 1998

NIFS-DATA-47 I. Murakami, K. Moribayashi and T. Kato,
Effect of Recombination Processes on FeXXIII Line Intensities; May 1998

NIFS-DATA-48 Zhijie Li, T. Kenmotsu, T. Kawamura, T. Ono and Y. Yamamura,
Sputtering Yield Calculations Using an Interatomic Potential with the Shell Effect and a New Local Model; Oct. 1998

NIFS-DATA-49 S. Sasaki, M. Goto, T. Kato and S. Takamura,
Line Intensity Ratios of Helium Atom in an Ionizing Plasma; Oct. 1998

NIFS-DATA-50 I. Murakami, T. Kato and U. Safronova,
Spectral Line Intensities of NeVII for Non-equilibrium Ionization Plasma Including Dielectronic Recombination Processses; Jan 1999

NIFS-DATA-51 Hiro Tawara and Masa Kato,
Electron Impact Ionization Data for Atoms and Ions -up-dated in 1998-; Feb. 1999

NIFS-DATA-52 J.G. Wang, T. Kato and I. Murakami,
Validity of n^{-3} Scaling Law in Dielectronic Recombination Processes; Apr 1999

NIFS-DATA-53 J.G. Wang, T. Kato and I. Murakami,
Dielectronic Recombination Rate Coefficients to Excited States of He from He^{+}; Apr. 1999

NIFS-DATA-54 T. Kato and E. Asano,
Comparison of Recombination Rate Coefficients Given by Empirical Formulas for Ions from Hydrogen through Nickel; June 1999

NIFS-DATA-55 H.P. Summers, H. Anderson, T. Kato and S. Murakami,
Hydrogen Beam Stopping and Beam Emission Data for LHD; Nov. 1999

NIFS-DATA-56 S. Born, N. Matsunami and H. Tawara,
A Simple Theoretical Approach to Determine Relative Ion Yield (RIY) in Glow Discharge Mass Spectrometry (GDMS); Jan. 2000

NIFS-DATA-57 T. Ono, T. Kawamura, T. Kenmotsu, Y. Yamamura,
Simulation Study on Retention and Reflection from Tungsten Carbide under High Fluence of Helium Ions; Aug. 2000

NIFS-DATA-58 J.G. Wang, M. Kato and T. Kato,
Spectra of Neutral Carbon for Plasma Diagnostics; Oct. 2000

NIFS-DATA-59 Yu V. Ralchenko, R. K. Janev, T. Kato, D.V. Fursa, I. Bray and F.J. de Heer
Cross Section Database for Collision Processes of Helium Atom with Charged Particles.
I. Electron Impact Processes; Oct. 2000

NIFS-DATA-60 U.I. Safronova, C. Namba, W.R. Johnson, M.S. Safronova,
Relativistic Many-Body Calculations of Energies for n = 3 States in Aluminiumlike Ions; Jan. 2001

NIFS-DATA-61 U.I. Safronova, C. Namba, I. Murakami, W.R. Johnson and M.S. Safronova,
E1,E2, M1, and M2 Transitions in the Neon Isoelectronic Sequence; Jan. 2001

NIFS-DATA-62 R. K. Janev, Yu.V. Ralchenko, T. Kenmotsu,
Unified Analytic Formula for Physical Sputtering Yield at Normal Ion Incidence; Apr. 2001